

Effect of the Melt Viscoelastic Behavior of Components on the Morphology Development of Polymer Blends in a Twin-Screw Extruder

L. Barangi, H. Nazockdast, F. Afshar Taromi

Polymer Engineering Department, Amirkabir University of Technology, Tehran, Iran

Received 9 May 2007; accepted 23 October 2007

DOI 10.1002/app.27596

Published online 20 February 2008 in Wiley InterScience (www.interscience.wiley.com).

ABSTRACT: The aim of this work was to study the role of effective parameters in the morphology evolution of polymer blends in a twin-screw extruder with an emphasis on the effects of the melt viscoelastic properties of the blend components, screw speed, and flow field changes along the extruder. Two sets of blend samples based on polypropylene/polyamide 6 with the same composition (90/10) and polypropylene matrix but with two polyamide 6 grades differing in their viscoelastic properties were considered. The effect of the compatibilizer (maleic anhydride grafted polypropylene) was also investigated. The morphology of the blend samples were studied with scanning electron microscopy, and the melt linear viscoelastic properties of the samples were measured with a rheometric mechanical spectrometer. The melt-blending processes were carried out in a modular twin-screw extruder. The

trend of the polyamide dispersed particle size changing with increasing screw speed was found to be different for the two types of blends. Considering of the role of the compatibilizer in coalescence, this could mainly be attributed to the different melt viscoelastic properties of the blend constituents. Similar explanations were given for the morphological changes that occurred along the screw. It was demonstrated that the viscosity ratio of the blend components is not necessarily the only material-dependent parameter that affects the dispersed particle size: the viscoelastic properties (particularly the flow-induced elasticity ratio) of the blend components can also play a significant role in determining the particle size distribution. © 2008 Wiley Periodicals, Inc. *J Appl Polym Sci* 108: 2558–2563, 2008

Key words: blends; morphology; viscoelastic properties

INTRODUCTION

Blending polymers with different physical properties presents the possibility of enhancing the overall properties of a material through a synergistic combination of the desirable properties of each compound in the system. As most polymers are thermodynamically immiscible, their blending usually leads to the formation of disperse systems in which the minor component is dispersed in the matrix phase. The viscosity ratio, shear rate, and flow field are among the important parameters that determine the size and size distribution of the dispersed phase in polymer blends.^{1,2} In compatibilized blends, the type and concentration of the compatibilizer also play a significant role in determining the dispersed particle size.^{3,4} Moreover, in some compatibilized polymer blends, an emulsion-in-emulsion morphology has also been reported.⁵ On the other hand, the size and size distribution of the dispersed phase have strong effects on the mechanical properties of the blends.

Therefore, it is generally desirable to generate blends with well-defined and reproducible morphologies.

The efficient mixing action of tightly intermeshing, corotating twin-screw extruders enables these extruders to be used as the most important tools for the production of polymer blends.⁶ During the past decade, numerous research groups have investigated the morphology development of polymer blends in twin-screw extruders.^{7–14} Despite much effort, we still do not have a clear understanding of the morphology evolution in immiscible polymer blends during compounding in twin-screw extruders.

The typical screw profile usually consists of an initial melting or plastification section followed by a conveying section and subsequently a mixing section to homogenize the polymer melt. It has been shown that the blend morphology in an extruder undergoes only small changes after the initial softening stage in the melting zone.¹⁵ However, the final morphology determining the characteristics of the end product is largely controlled by the design of the geometry, the selection of the processes conditions, and consequently the flow conditions in the last section of the extruder and in the following die. The aim of this work was to study the effect of the melt viscoelastic properties of the components on the morphology

Correspondence to: H. Nazockdast (nazdast@aut.ac.ir).

TABLE I
Characteristics of the Blend Components

Polymer	Melt flow rate at 230°C (g/10 min)	Viscosity number (cm ³ /gr)	Zero shear viscosity at 260°C (Pa s)	Maleic anhydride content (wt %)
PP	16	—	890	—
PA6(1)	—	150	620	—
PA6(2)	—	320	5120	—
PP-g-MAH	24	—	330	0.5

evolution of polypropylene (PP)/polyamide 6 (PA6) blends in a twin-screw extruder.

EXPERIMENTAL

Materials

A commercial isotactic PP (Poliran-V30S), supplied by Arak Petrochemical Co. (Iran), was used as the matrix. Two grades of PA6, Bergamid B700-20 from Poly One (Germany) [which is called PA6(1)] and Ultramid B5 from BASF (Germany) [which is called PA6(2)], were used as the minor phase. A commercial grade of maleic anhydride grafted polypropylene (PP-g-MAH), manufactured by Dupont (United Kingdom) (Fusabond 511D), was used as the compatibilizer. Table I shows the characteristics of these polymers.

Blend preparation

Table II lists the compositions of the blends investigated. The PA6 granules were dried in a vacuum oven at 80°C for 24 h before blending. All the samples were prepared in a Brabender (Germany) DSE25 intermeshing, corotating twin-screw extruder with a length/diameter ratio of 30. The screw configuration is described in Figure 1. The throughput of the extruder was kept constant by means of an independent dosing system. The samples were prepared at three different screw speeds (100, 150, and 200 rpm). The temperature of the barrel feed section was maintained at 20°C, and the rest of the barrel was kept at 260°C. The morphology evolution of the blends along the extruder was studied through the examination of samples collected at different zones of the extruder, as described in Figure 1. The samples, taken from the extruder during the steady-state operation, were immediately cooled in liquid nitrogen to preserve the morphology that developed in the extruder.

Rheological studies

The melt linear viscoelastic properties of the blend components and the blend samples were measured with a Paar Physica (Austria) USD200 rheometric mechanical spectrometer equipped with parallel-plate geometry with a diameter of 25 mm at a strain of 1% and temperature of 260°C. The flow behavior

of the blend components was also obtained with a capillary rheometer and a rheometric mechanical spectrometer.

Morphology study and image analysis

The morphological studies were performed on the cryogenically fractured surface of the samples. To achieve good contrast for quantitative measurements of the dispersed particle size, the dispersed PA6 phase was etched by submersion of the samples in 98% formic acid for 4 h. The etched samples were then sputter-coated with gold and examined by scanning electron microscopy (SEM). The particle size distribution was determined with image analysis performed on SEM micrographs. The equivalent diameter (d) was calculated on the basis of the particle area with eq. (1):

$$d = \sqrt{\frac{4}{\pi} \cdot A_{\text{particle}}} \quad (1)$$

where A_{particle} represents the area of the dispersed particle. From the values of d obtained in this way, the number-average diameter (d_n) was formed as follows:

$$d_n = \frac{\sum d_i}{n} \quad (2)$$

where d_i represents the equivalent diameter of each particle and n is the number of particles.

RESULTS AND DISCUSSION

Figure 2 shows the results of the viscosity measured as a function of the shear rate for the blend constituents at a temperature of 260°C.

TABLE II
Compositions of the Blends

Sample	PP content (wt %)	PA6 content (wt %)	Compatibilizer content (wt %)
B1	90	10% PA6(1)	0
B2	90	10% PA6(2)	0
CB1	89.5	10% PA6(1)	0.5

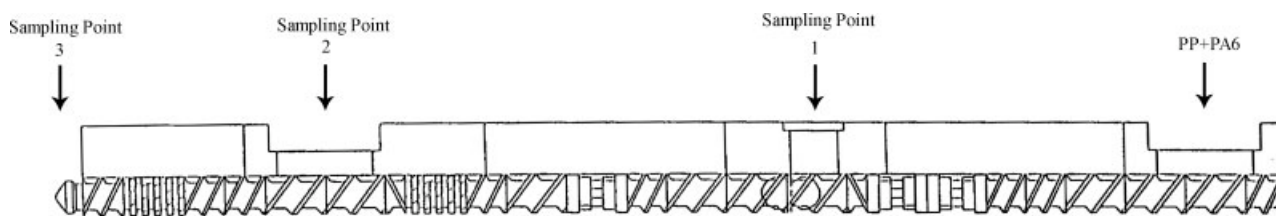


Figure 1 Screw configuration and sampling locations.

The results of the viscosity ratio, η_d/η_m (where η_d and η_m are the viscosities of the dispersed phase and matrix, respectively), as a function of the shear rate at a temperature of 260°C for the blend systems are shown in Figure 3. Although the viscosity ratio of blend B1 was lower than 4 in the whole range of shear rates, the viscosity ratio was higher than 5 for blend B2. It has been shown^{16,17} that droplet breakup is easiest when the viscosity ratio tends to 1 and d_n of the dispersed particles is enlarged at a viscosity ratio greater than 1. Grace¹⁶ correlated the critical capillary number with the viscosity ratio and showed that the droplet breakup process is promoted at viscosity ratios between 0.1 and 1 and that a drop will not break if the viscosity ratio is greater than 3.5 for Newtonian systems subjected to a simple shear flow field. It has also been reported that in polymer systems, the droplets experience not only dissipative (viscous) forces but also the deformation-resisting forces arising from the elasticity.^{2,18,19} Therefore, the mechanism of droplet deformation and breakup is quite different in viscoelastic systems from that in Newtonian systems. Most studies^{15,18–22} have reported that matrix elasticity assists with the deformation of the droplet, whereas the droplet elasticity resists the drop deformation. Therefore, the elasticity of the blend components can also play a role in determining the droplet size in the polymer melt blending process.

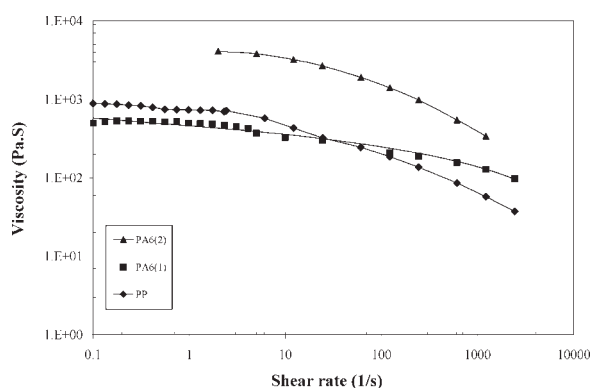


Figure 2 Viscosity versus the shear rate for the blend components.

Figure 4 shows the results of the storage modulus as a function of frequency for the blend components. The storage modulus ratio (G'_d/G'_m) of the blends as a function of frequency is shown in Figure 5. By comparing these results, one may notice that G'_d/G'_m (storage modulus of dispersed phase and matrix, respectively) of blend B2 is greater than unity and decreases with increasing angular frequency, tending to 1 at a frequency around 1000 (1/s), whereas for blend B1, this ratio is much lower than 1 and increases with the angular frequency.

From these results, one may realize that for blend B1, the droplet breakup process is expected to be easier at a low shear rate, whereas a reverse result may be expected for blend B2. These results also suggest a larger particle size for B2 compared to B1 because of its much greater viscosity ratio.

Figure 6 shows typical SEM micrographs of blend B1 collected from the same screw positions (zone 1) at different screw speeds (shear rates). From that and the results shown in Figure 7, it can be noted the polyamide particle size increases from 0.8 to 4 μm as the screw speed increases from 150 to 200. Following the capillary number, increasing the screw speed is expected to decrease the particle size. However, as can be seen in Figure 3 for blend B1, because of pseudoplastic behavior of the components, increasing the shear rate increases the viscosity ratio from 0.8 to 2.6 when the shear rate increases from 5 to 2000 (1/s). The melt elasticity ratio of the blend components is also increased with increasing

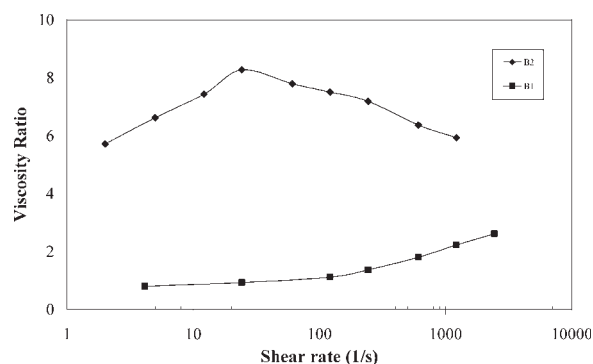


Figure 3 Viscosity ratios of the blends versus the shear rate.

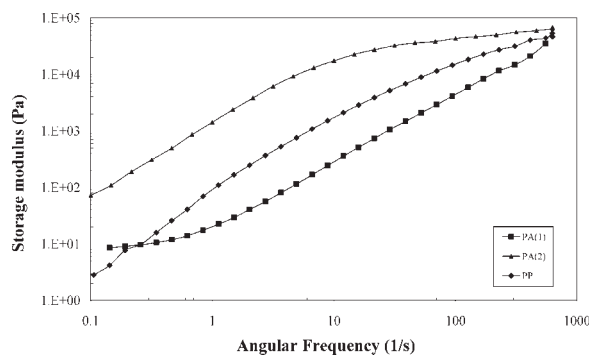


Figure 4 Storage modulus versus the frequency for PP, PA6(1), and PA6(2).

screw speed. These viscoelastic variations act against the droplet breakup process and hence lead to enlargement of the particle size. Increasing the screw speed can also increase the probability of coalescence, leading to increasing dispersed particle size.

Figure 7 also shows the variation of the dispersed particle size against the screw speed (shear rate) for blend B2. In B2, in contrast to B1, the average particle size is reduced from 2.8 to 1.1 μm as the screw speed increases from 150 to 200 rpm. From the results shown in Figures 3 and 5, one may notice that in blend B2, in contrast to blend B1, the viscosity ratio is too high (>3.5) in the whole range of shear rates, and it does not play a significant role in the droplet breakup process; however, the melt elasticity ratio of this sample is reduced with the shear rate and tends to 1. This is in favor of the droplet breakup process and will lead to a smaller particle size.

Figure 8 compares the variation of the polyamide particle diameter of blend B1 collected at three different screw positions for two different screw speeds (100 and 200 rpm). For blend B1 prepared at the screw speed of 100 rpm, the particle size diameter of the sample increases from zone 1 to zone 3, whereas a reverse trend of the variation of the particle size

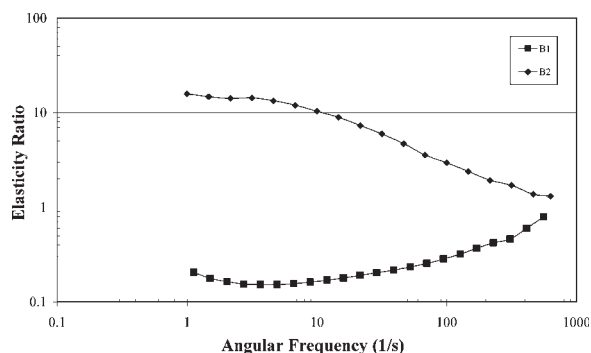


Figure 5 Elasticity ratios of the blends versus the frequency.

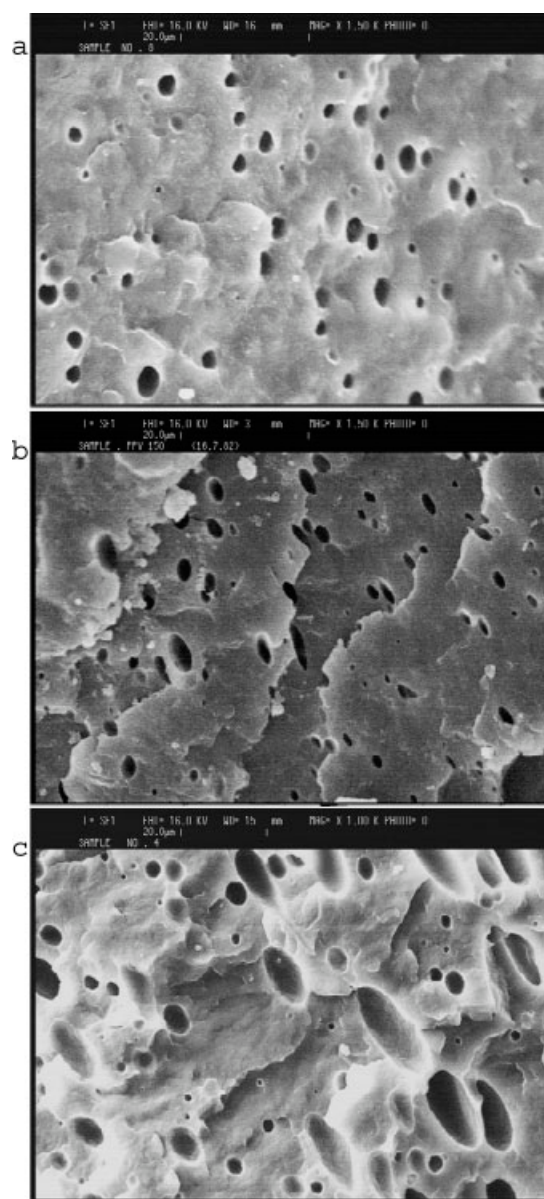


Figure 6 SEM micrographs of blend B1 at different screw speeds: (a) 100, (b) 150, and (c) 200 rpm.

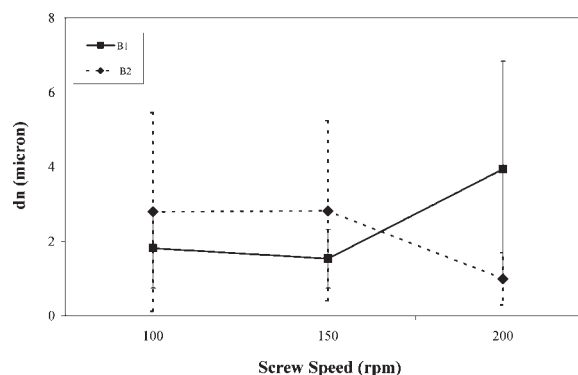


Figure 7 Mean particle size (with standard deviations) versus the screw speed for B1 and B2.

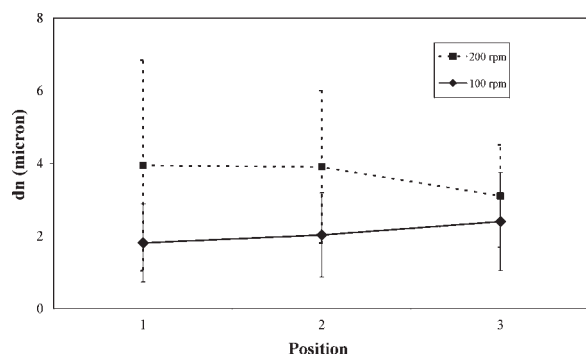


Figure 8 Variation of d_n (with standard deviations) measured along the screw for blend B1 (100 and 200 rpm).

with the position is observed for the same sample prepared at the screw speed of 200 rpm. At the screw speed of 100 rpm, the melt elasticity of the blend constituents is very low; therefore, it seems that coalescence is dominating the particle size. However, at the screw speed of 200 rpm, the elasticity of the components is high, and so the reduction of the particle size from zone 1 to zone 3 can be attributed to the reduction of the elasticity ratio.

Figure 9 shows the variation of the particle diameter along the extruder for blend B2 at screw speeds of 100 and 200 rpm. As discussed earlier for B2, the viscosity ratio is higher than 3.5 in the whole range of shear rates; therefore, increasing the particle size of this sample from zone 1 to zone 3 can be attributed only to the increase of the elasticity ratio.

Figure 10 presents a typical SEM macrograph of the compatibilized blend (CB1). The particle size of the sample was found to be around 0.6 μm , which was much smaller than those obtained in the uncompatibilized blend (1.8 μm).

Figure 11 shows the variation of the particle size with increasing screw speed for blend CB1 collected from zone 1 of the extruder. These results showed the same trend for the variation of the particle size

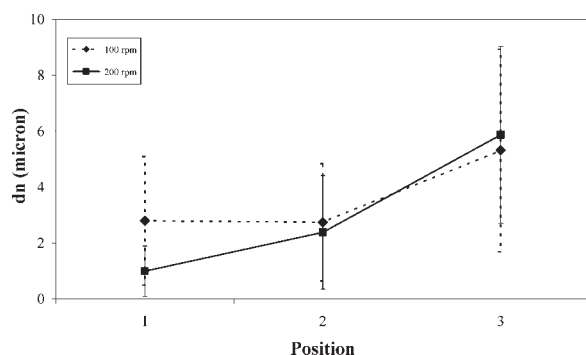


Figure 9 Variation of d_n (with standard deviations) measured along the screw for blend B2 (100 and 200 rpm).

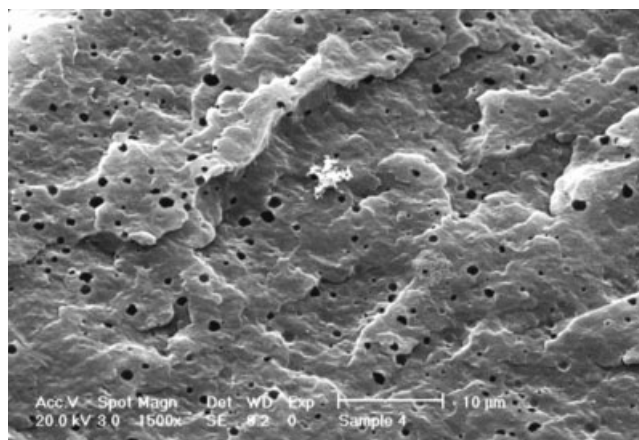


Figure 10 SEM micrograph of CB1 (screw speed = 100 rpm, position 1).

with the screw speed as that obtained for blend B1. As the compatibilization process reduces the coalescence of droplets, the similar effect of the screw speed on the particle size observed for compatibilized and uncompatibilized samples supports the idea that an increase in the elasticity of the dispersed phase with the screw speed is the dominating parameter.

The variation of the particle size along the extruder at three different screw speeds for blend CB1 is shown in Figure 12. The extent of reducing the polyamide particle size of compatibilized samples along the screw was found to be lower compared to that of uncompatibilized samples. In compatibilized samples, the coalescence has no appreciable effect on increasing the particle size along the extruder, and the elasticity ratio is the controlling parameter. In other words, the extent of the variation of the particle size along the extruder is dependent on the screw speed.

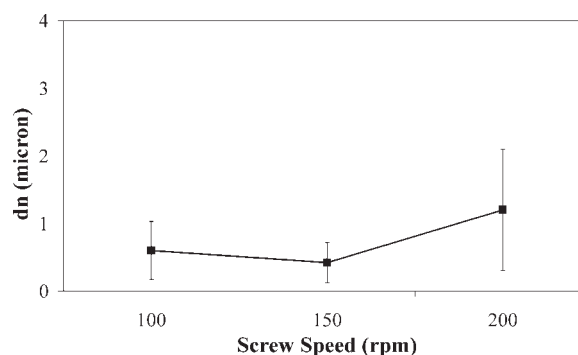


Figure 11 Mean particle size (with standard deviations) versus the screw speed for CB1.

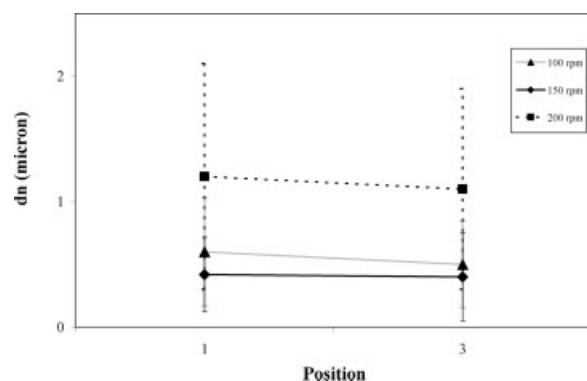


Figure 12 Variation of d_n (with standard deviations) measured along the screw for blend CB1 (100, 150, and 200 rpm).

CONCLUSIONS

It has been shown that increasing the screw speed may not necessarily result in decreasing the particle size of the minor phase in immiscible polymer blends, but it can have different effects depending on the viscoelastic properties of the blend components. These blends also showed different trends of morphological changes along the extruder. The presence of PP-grafted MA in the blends had a similar effect in the morphology of the two blends. It has been demonstrated that the viscosity ratio of the components is not necessarily the only parameter that determines the particles size of the dispersed phase: the elasticity ratio of the blend constituents

can also play a significant role in controlling the dispersed particle size.

References

1. Utracki, L. A. *Two-Phase Polymer Systems*; Hanser: Munich, 1991.
2. Utracki, L. A.; Shi, Z. H. *Polym Eng Sci* 1992, 32, 1824.
3. Filippone, G.; Netti, P. A.; Acierno, D. *Polymer* 2007, 48, 564.
4. Filippi, S.; Minkova, L.; Dintcheva, N.; Narducci, P.; Magagnini, P. *Polymer* 2005, 46, 8054.
5. Shi, D.; Hu, G. H.; Ke, Z.; Li, R. K. Y.; Yin, J. *Polymer* 2006, 47, 4659.
6. White, J. L. *Twin Screw Extrusion—Technology and Principles*; Hanser: Munich, 1990.
7. Lee, J. K.; Han, C. D. *Polymer* 2000, 41, 799.
8. Franzheim, O.; Stephan, M.; Rische, T. *Adv Polym Technol* 1997, 16, 1.
9. Potente, H.; Bastian, M.; Gehring, A.; Stephan, M.; Potschke, P. *J Appl Polym Sci* 2000, 76, 708.
10. Potente, H.; Bastian, M.; Bergemann, K. *Polym Eng Sci* 2001, 41, 222.
11. Potente, H.; Krawinkel, S.; Bastian, M. *J Appl Polym Sci* 2001, 82, 1986.
12. Machado, A. V.; Covas, J. A.; Walet, M.; Van Duin, M. *J Appl Polym Sci* 2001, 80, 1535.
13. Barangi, L.; Nazockdast, H. *Int Congr Rheol* 2004, 24, 36.
14. Potluri, R.; Todd, D.; Gogos, C. *Adv Polym Technol* 2006, 25, 81.
15. Sundararaj, U.; Dori, Y.; Macosko, C. W. *Polymer* 1995, 36, 1957.
16. Grace, H. P. *Chem Eng Commun* 1982, 14, 225.
17. Wu, S. *Polym Eng Sci* 1987, 27, 335.
18. Ghodgonrar, P. G.; Sandararaj, U. *Polym Eng Sci* 1996, 36, 1656.
19. Levitt, L.; Macosko, C. W.; Pearson, S. D. *Polym Eng Sci* 1996, 36, 1647.
20. Lin, B.; Sundararaj, U. *Polym Eng Sci* 2003, 43, 891.
21. Mighri, F.; Carreau, P. J.; Aji, A. *J Rheol* 1998, 42, 1477.
22. Mighri, F.; Huneault, M. A. *J Rheol* 2001, 45, 738.